Modeling ion permeation through batrachotoxin-modified Na^+ channels from rat skeletal muscle with a multi-ion pore

Arippa Ravindran,* Hubert Kwiecinski,* Osvaldo Alvarez,‡ George Eisenman,§ and Edward Moczydlowski*

*Department of Pharmacology and Department of Cellular and Molecular Physiology, Yale University School of Medicine, New Haven, Connecticut 06510; ‡Departamento de Biologia, Facultad de Ciencias, Universidad de Chile, Las Palmeras 3425, Casilla 653, Santiago, Chile; and §Department of Physiology, University of California School of Medicine, Los Angeles, California 90024

ABSTRACT The mechanism of ion permeation through Na^+ channels that have been modified by batrachotoxin (BTX) and inserted into planar bilayers has been generally described by models based on single-ion occupancy, with or without an influence of negative surface charge, depending on the tissue source. For native Na^+ channels there is evidence suggestive of a multi-ion conduction mechanism. To explore the question of ion occupancy, we have reexamined permeation of Na^+, Li^+, and K^+ through BTX-modified Na^+ channels from rat skeletal muscle. Single-channel current–voltage (I-V) behavior was studied in neutral lipid bilayers in the presence of symmetrical Na^+ concentrations ranging from 0.5 to 3,000 mM. The dependence of unitary current on the mole fraction of Na^+ was also examined in symmetrical mixtures of Na^+–Li^+ and Na^+–K^+ at a constant total ionic strength of 206 and 2,006 mM. The dependence of unitary conductance on symmetrical Na^+ concentration does not exhibit Michaelis-Menten behavior characteristic of single-ion occupancy but can be simulated by an Eyring-type model with three barriers and two sites (3B2S) that includes double occupancy and ion–ion repulsion. Best-fit energy barrier profiles for Na^+, Li^+, and K^+ were obtained by nonlinear curve fitting of I-V data using the 3B2S model. The Na^+–Li^+ and Na^+–K^+ mole-fraction experiments do not exhibit an anomalous mole-fraction effect. However, the 3B2S model is able to account for the biphasic dependence of unitary conductance on symmetrical [Na^+] that is suggestive of multiple occupancy and the monotonic dependence of unitary current on the mole fraction of Na^+ that is compatible with single or multiple occupancy. The best-fit 3B2S barrier profiles also successfully predict bi-ionic reversal potentials for Na^+–Li^+ and Na^+–K^+ in both orientations across the channel. Our experimental and modeling results reconcile the dual personality of ion permeation through Na^+ channels, which can display features of single or multiple occupancy under various conditions. To a first approximation, the 3B2S model developed for this channel does not require corrections for vestibule surface charge. However, if negative surface charges of the protein do influence conduction, the conductance behavior in the limit of low [Na^+] does not correspond to a Gouy-Chapman model of planar surface charge.

INTRODUCTION

Voltage-activated ion channels comprise a superfamily of structurally related membrane proteins that include three distinct subfamilies selective for Na^+, K^+, or Ca^{2+}. How do the respective Na^+, K^+, and Ca^{2+} channel members of this protein superfamily efficiently recognize their preferred ion for conduction? At the molecular level, the answer to this question requires identification and resolution of the pore structures for these proteins. In a complementary fashion, mechanistic insight to this problem requires a detailed analysis of function. The current–voltage (I-V) behavior of ion permeation may be expected to reveal significant features of the underlying energy profiles that ions experience as they pass through these three types of channels. Consistent with this expectation, a review of the literature on Na^+, K^+, and Ca^{2+} channels suggests that they share a common mechanism of conduction involving single-file movement through a multi-ion pore, i.e., a pore that can be simultaneously occupied by more than one permeant ion (for reviews see Begenisich, 1987; Tsien et al, 1987; Yellen, 1987).

Conceptual understanding of many phenomena associated with permeation through voltage-activated channels has been achieved by the application of Eyring rate theory to a linear chain of ion binding sites as a discrete kinetic model for ion transport (for review, see Eisenman and Horn, 1983). The deviation from ion independence observed for macroscopic Na^+ currents of frog myelinated nerve was first modeled as a four-barrier, three-site (4B3S) system that limited occupancy of the pore to one ion at a time (Hille, 1975). However, in order to explain bi-ionic permeability ratios that vary with the concentration of the internal permeant ion for squid axon Na^+ currents (Chandler and Meves, 1965; Cahalan and Begenisich, 1976; Ebert and Goldman, 1976), Begenisich and Cahalan (1980*a*,*b*) introduced a

Address correspondence to Dr. Edward Moczydlowski, Department of Pharmacology, Yale University School of Medicine, 333 Cedar St., New Haven, CT 06510.

A. Ravindran's present address is Department of Neuroscience, Johns Hopkins University School of Medicine, Baltimore, MD 21205.

H. Kwiecinski's present address is Department of Neurology, Medical Academy of Warsaw, 02-097 Warsaw, Poland.

0006-3495/91/02/494/15 $2.00

three-barrier, two-site (3B2S) model that allowed for simultaneous occupancy of the two sites. A similar 3B2S model including ion–ion repulsion was shown to explain several distinctive features of macroscopic currents through voltage-activated K^+ channels (Hille and Schwarz, 1978). These properties include a unidirectional flux ratio exponent > 1.0, a large effective valence ($z\delta > 1.0$) of monovalent blocking ions such as Cs^+, and an anomalous minimum in the mole-fraction dependence of currents measured in mixtures of certain permeant ions. Likewise, analysis of macroscopic measurements of monovalent and divalent cation permeation through L-type Ca^{2+} channels also led to a 3B2S model with double occupancy and repulsion (Almers and McCleskey, 1984; Hess and Tsien, 1984).

More recent investigations of actual unitary currents through single voltage- and Ca^{2+}-activated K^+ channels (Eisenman et al, 1986; Cecchi et al, 1987) and L-type Ca^{2+} channels (Friel and Tsien, 1989; Yue and Marban, 1990) have invoked multiple ion occupancy as a necessary feature of minimal barrier models for permeation through these particular channels. However, consensus on a barrier model for ion permeation through single voltage-activated Na^+ channels has not yet been achieved. Detailed analysis of permeation through single Na^+ channels is especially difficult because of the brief openings of normally inactivating channels. Thus, many studies have taken advantage of drugs, reagents, or enzymes that slow kinetics of inactivation or prolong Na^+ channel opening. In a study of single tetramethrin-modified Na^+ channels of neuroblastoma cells, Yamamoto et al. (1984) simulated the I-V behavior in the absence and presence of the external blocking ion, Ca^{2+}, by a 4B3S single-ion occupancy model similar to that previously used for macroscopic Na^+ currents (Hille, 1975). Analogous experiments with cardiac Na^+ channels were also interpreted on the basis of the same 4B3S single-occupancy model (Sheets et al., 1987; Nilius, 1988). The use of single-occupancy models for Na^+ channels has been justified by the finding that flux-ratio exponents of currents through Na^+ channels approach unity under physiological conditions (Begenisich and Busath, 1981; Busath and Begenisich, 1982), suggesting that Na^+ channels are normally occupied by one ion at a time. However, a variety of blocking experiments have revealed striking interactions between Na^+ ions and internal cationic blocking drugs that are consistent with the possibility of multiple ion occupancy (Shapiro, 1977; Cahalan and Almers, 1979; Danko et al., 1986; Wang, 1988).

To clarify the disparity between the evidence for multi-ion behavior and the application of single-ion conduction models, it is necessary to demonstrate at the single-channel level that Na^+ channels are capable of simultaneously binding more than one permeant ion. Na^+ channels modified by batrachotoxin (BTX) and incorporated into planar lipid bilayers (Krueger et al., 1983) are a useful system for examining this question. With this method, accurate measurements of unitary currents over a wide range of ionic concentrations can be made on Na^+ channels in bilayers composed of neutral phospholipids that obviate possible effects of negative surface charge due to anionic lipids surrounding the channel (Apell et al., 1979; Bell and Miller, 1984; Moczydlowski et al., 1985). Permeation of Na^+ through such BTX-modified Na^+ channels from rat skeletal muscle has been described as a Michaelis-Menten dependence, $g = g_{max}[Na^+]/\{K_m + [Na^+]\}$, of unitary conductance (g) on Na^+ concentration in the range of 5 to 500 mM symmetrical NaCl or Na-acetate, with a maximal conductance (g_{max}) of 21 pS and a Michaelis-Menten constant (K_m) of 6.5 to 8 mM (Moczydlowski et al., 1984; Garber and Miller, 1987). Assuming single-ion occupancy, Garber (1988) was able to partially account for the I-V behavior of BTX-modified Na^+ channels from rat muscle in the presence of symmetrical and bi-ionic solutions of Na^+, Li^+, and K^+. Analogous experiments on BTX-modified Na^+ channels from squid optic nerve in planar bilayers (Behrens et al., 1989) showed very similar Michaelis-Menten behavior to that of rat muscle Na^+ channels, and g_{max} = 23 pS and K_m = 11 mM. In contrast to these results, the conductance-concentration behavior for BTX-modified Na^+ channels from dog brain in planar bilayers (Green et al., 1987*a*) and normal or BTX-modified Na^+ channels from squid axon, measured by the cut-open axon technique (Correa et al,. 1991), deviate from Michaelis-Menten behavior in the low Na^+ concentration limit. In these latter two cases, the process of Na^+ permeation was modeled either as a singly occupied channel with negative surface charge in the vicinity of the channel vestibules (Green et al., 1987*a*) or as a singly or doubly occupied channel with negative surface charge (Correa et al., 1991).

To further investigate the question of single- vs. multi-ion occupancy, we have reexamined permeation through BTX-modified Na^+ channels from rat muscle in the presence of Na^+, Li^+, and K^+. To test more rigorously for deviations from Michaelis-Menten behavior, the I-V behavior of this channel was studied over a wide range of symmetrical Na^+ concentration. In addition, we examined I-V behavior at fixed ionic strength (0.2 and 2 M) in the presence of symmetrical mixtures of Na^+/Li^+ and Na^+/K^+ to look for the presence of an anomalous mole-fraction effect (Neher, 1975; Eisenman et al, 1977; Sondblom, et al. 1977) that would substantiate multi-ion conduction. Although our experiments with mixtures of two permeant ions did not reveal this latter effect, the observed biphasic conductance–concentration relation

for Na^+ and the monotonic conductance behavior in mixtures of permeant ions can be simulated by 3B2S energy barrier profiles that assume double occupancy, ion–ion repulsion, and the absence of negative surface charge.

MATERIALS AND METHODS

Planar bilayer recording

Procedures for incorporating BTX-modified Na^+ channels from plasma membrane preparations of rat skeletal muscle or canine heart into planar bilayers have been described previously (Ravindran et al., 1991; Schild and Moczydlowski, 1991). Phospholipid bilayers were formed from a mixture (4:1) of bovine brain phosphatidylethanolamine1,2-diphytanoylphosphatidylcholine (Avanti Polar Lipids, Inc., Birmingham, AL). Bilayers were formed by spontaneous thinning of a solution (25 mg/ml in decane) of the above lipids painted over a 200-μm hole in a polystyrene partition (Warner Instruments Corp., Hamden, CT).

In bilayer experiments with symmetrical NaCl concentrations in the range of 50 to 3,000 mM, Na^+ channels were incorporated by addition of plasma membranes and 0.2 μM BTX to one side (*cis*) of a bilayer formed in the presence of the final NaCl concentration. For lower NaCl concentrations, Na^+ channels were first incorporated in the presence of 100 mM symmetrical NaCl and both chambers were extensively perfused (20–30 vol with stirring) with low Na^+ solution on both sides. Perfusion was accomplished with an infusion-withdrawal pump (model 94, Harvard Apparatus, South Natick, MA). For some of the mole-fraction experiments at high LiCl or KCl concentrations, it was also necessary to incorporate channels in the presence of NaCl on the *cis* side followed by perfusion with the desired final solution.

Unitary Na^+ currents were recorded at ambient temperature (21–24°C) with either a simple homebuilt amplifier based on patch-clamp design or a patch-clamp amplifier (model 8900, Dagan Corp., Minneapolis, MN). The amplifier headstage was connected with two Ag-AgCl wire electrodes to two separate wells containing 500 mM KCl. The wells were separately connected to the bilayer chambers with small capillary bridges filled with 0.2 M KCl and 1 mM EDTA in 2% agar.

Voltage signs are referenced according to the physiological convention (extracellular ground). In the majority of experiments, Na^+ channels incorporated with the extracellular side facing the chamber containing the membrane preparation. However, channel orientation was verified for every bilayer by addition of a guanidinium toxin (tetrodotoxin, saxitoxin, or decarbamoylsaxitoxin). These toxins produce discrete blocking events in BTX-modified Na^+ channels only when present on the extracellular side. Such toxins also facilitate accurate measurements of unitary currents from well-resolved transitions between the open and closed (or blocked) state. The concentration of added guanidinium toxin ranged from 1 nM to 1 μM, depending on the toxin and Na^+ channel subtype (skeletal muscle vs. heart). The toxin concentration was based on that which produces ~50% blocking probability at 0 mV as determined in previous studies (Guo et al., 1987; Ravindran and Moczydlowski, 1989).

Since all experiments were performed in the presence of symmetrical electrolyte solutions on both sides of the bilayer, the absolute reversal potential is 0 mV. This permitted us to correct accurately for residual electrode asymmetry and junction potentials by subtraction of observed nonzero reversal potentials from applied potentials. Such corrections of applied voltage were generally <5 mV. Absolute conductance values were also calibrated with respect to a 10 GΩ 1% resistor. This latter correction was $<3\%$. Measurements of unitary conductance were not corrected for small variations in room temperature (21–24°C).

Bilayer solutions

For investigation of conductance vs. $[Na^+]$ behavior, electrolyte solutions symmetrically bathing both sides of the bilayer were designed to cover a range of 0.5 to 3,000 mM Na^+ as the predominant monovalent cation. The chelating agent, EDTA, was included to ensure the virtual absence of uncomplexed divalent cations, which are known to block voltage-dependent Na^+ channels (Ravindran et al., 1991). At NaCl concentrations >50 mM, the buffer was 10 mM 3-(*N*-morpholino)propanesulfonic acid (MOPS) and 0.2 mM EDTA (free acid), with NaCl concentrations ranging from 50 to 3,000 mM, and brought to pH 7.4 by addition of 6 mM NaOH. At lower Na^+ concentrations, the concentration of MOPS was lowered so that Na^+ and its counterions provided the overwhelming contribution to ionic strength. Thus, in the range of 2 to 20 mM total Na^+, the solution consisted of 2 mM MOPS; 1.2 mM NaOH; 0.1 mM EDTA, pH 7.4; and 0.8, 3.8, 8.8, or 18.8 mM NaCl. For 1 mM total Na^+, the buffer was prepared by titration of 1 mM standardized NaOH and 0.1 mM EDTA to pH 7.4 with MOPS. For 0.5 mM total Na^+, 0.5 mM NaOH and 0.05 mM EDTA were titrated to pH 7.4 with MOPS. For rat muscle Na^+ channels, single-channel I-V curves were also measured in the following alternative solutions for 2 and 5 mM Na^+: 0.5 mM Na_4(EDTA), to pH 7.4 with MOPS and 0.5 mM Na_4(EDTA), 3 mM NaCl to pH 7.4 with MOPS. The pH of all solutions was checked periodically to ensure that pH was held constant at 7.4 for all of the conductance measurements.

In a second type of experiment, single-channel I-V relations were measured in mixtures of Na^+/Li^+ and Na^+/K^+ at two fixed salt concentrations of 206 and 2,006 mM. The buffers for these experiments consisted of 10 mM MOPS, 0.2 mM EDTA, and 6 mM NaOH, pH 7.4, and various concentrations of LiCl or KCl ranging from 0 to 200 or 0 to 2,000 mM. Ionic strength was maintained constant in these solutions by addition of NaCl required to give total monovalent cation concentrations of 206 or 2,006 mM.

Salts and chemicals were reagent grade and the water was deionized by a Milli-Q system (Millipore Corp., Bedford, MA).

Measurement of single-channel I-V curves

The open-state current of BTX-modified Na^+ channels from rat muscle and canine heart was well defined over the whole $[Na^+]$ and voltage range of 0.5 to 3,000 mM Na^+ and ±70 mV. Unitary currents were measured at ±10-mV intervals directly from chart recordings taken at 10 or 20 cm/min (Microscribe recorder, model 4500, Houston Instruments, Austin, TX) and filtered at 20–100 Hz. Measurement of 5–10 channel openings per I-V point was automated with the aid of a digitizing tablet (model TG1017, Houston Instruments) and an LSI 1173 computer (Indec Systems, Sunnyvale, CA). By measuring only well-defined closures induced by guanidinium toxins, the standard error on an I-V data point was generally <0.05 pA with this method. The apparent reversal potential used for junction-potential correction and the zero-voltage conductance value were determined by linear regression analysis of I-V data in the voltage range of ±50 mV.

For the rat muscle channel, the conductance results in Fig. 4 are the mean of data from 3 to 14 bilayers at each Na^+ concentration, except for 56 and 3,006 mM Na^+, both of which are based on two bilayers each. Similarly, for the canine heart channel, we obtained 3–11 bilayers at each Na^+ concentration, except for 56 and 2,006 mM Na^+, which included two bilayers each. Fig. 3 illustrates I-V (Fig. 3 *A*) or conductance-voltage (Fig. 3 *B*) data from one representative bilayer

for different experiments at 12 different Na^+ concentrations. The results of Na/Li (see Fig. 6) and Na/K (see Fig. 8) mole-fraction experiments are generally based on two to four bilayers at each of the various ion mixtures. Figs. 5 and 7 show superimposed I-V data from two different bilayers at each ion mixture to illustrate bilayer-to-bilayer reproducibility.

Modeling of energy profiles

Calculations of net ionic currents from energy barrier diagrams followed methods similar to those outlined previously (Hille and Schwarz, 1978; Begenisich and Cahalan, 1980*a*) for a 3B2S channel with double occupancy and ion–ion repulsion as described in detail elsewhere (Alvarez et al., 1991). The adjustable parameters of the model are summarized by the energy diagram in Fig. 9, *top*. The energies of the unoccupied channel at zero voltage are defined by three peaks, *G1*, *G2*, and *G3*, and two wells, *U1* and *U2*, with the subscript referring to position with respect to the inside solution. The distances D1–D6 refer to the fraction of the electric field that separates peak and well positions as indicated in Fig. 9, with the requirement that $D1 + D2 + D3 + D4 + D5 + D6 = 1.0$. In addition to the above energy and distance parameters, there is also an interaction energy, *A*, that models the effects of ion–ion interactions (electrostatic and/or allosteric) by addition of an energy, A/d, to peaks and wells adjacent to an occupied well, where d is the electrical distance from the occupied well. For the case of two permeant ions, there are three adjustable *A* parameters: *A1* for the Na^+-Na^+ interaction, *A2* for the Li^+-Li^+ or K^+-K^+ interaction, and *A12* for mixed-ion interactions. The effect of applied voltage is modeled by addition of the zero-voltage energy to an electrical work term proportional to valence of the ion and electrical distance as in previous applications of barrier models for ion channels (e.g., Hille and Schwarz, 1978; Begenisich and Cahalan, 1980*a*). Rate constants for transitions between permissible states were formulated by the standard Eyring rate theory expression equal to the product of a preexponential term, kT/h, and an exponential function of the energy difference, $\exp(\Delta G/kT)$. A similar expression was used for bimolecular rate constants describing entry of ions from the internal or external solutions, except that the preexponential factor was also multiplied by the molar activity of the ion in solution divided by the molar concentration of water (55.5 M). Thus, the reference energy state that we use corresponds to that of a 55.5 M solution. To directly compare our energy values to models that use a 1 M reference state, 4.0 RT units must be added to our values. A program in FORTRAN code for automated calculation of peak and well energies, transition rate constants, net current, and nonlinear least-squares fitting of I-V data to best-fit parameters on an IBM-compatible computer has been described in detail (Alvarez et al., 1991) and is available from two of the authors, O. Alvarez or G. Eisenman.

To keep our modeling results consistent with the universal practice of using the Goldman-Hodgkin-Katz equation to compute permeability ratios from reversal potentials, we used single-ion activities instead of concentrations in all calculations using the 3B2S model. Such ion activities for Na^+, Li^+, and K^+ were calculated directly from solution activity coefficients, assuming single-ion coefficients to be the same as mean values. To compare the impact of using Na^+ activity vs. Na^+ concentration scales on the final energy parameters, minimum least-squares fitting of I-V curves for the case of symmetrical Na^+ was performed with both scales. The results of this exercise showed that the best-fit *G*, *U*, and *A* parameters obtained by using activity vs. concentration differed by $<6\%$ in all cases. Although the activity scale is used exclusively for all calculations, all ion concentrations given in the text and figures are total absolute concentrations for ease of discussion.

RESULTS

Fig. 1 illustrates current records from bilayers containing one to three BTX-modified Na^+ channels bathed in symmetrical solutions of low ionic strength ranging from 0.5 to 10 mM Na^+. The unitary conductance of such BTX-modified Na^+ channels from rat skeletal muscle increases in a nearly linear fashion over this range of low Na^+ concentration (e.g., Fig. 4). Fig. 2 shows current records obtained in the presence of symmetrical solutions of NaCl, LiCl, or KCl at 0.2 or 2.0 M concentration. Long-duration closing events in these experiments were induced by addition of decarbamoylsaxitoxin to the external side of the channel in order to clearly define the

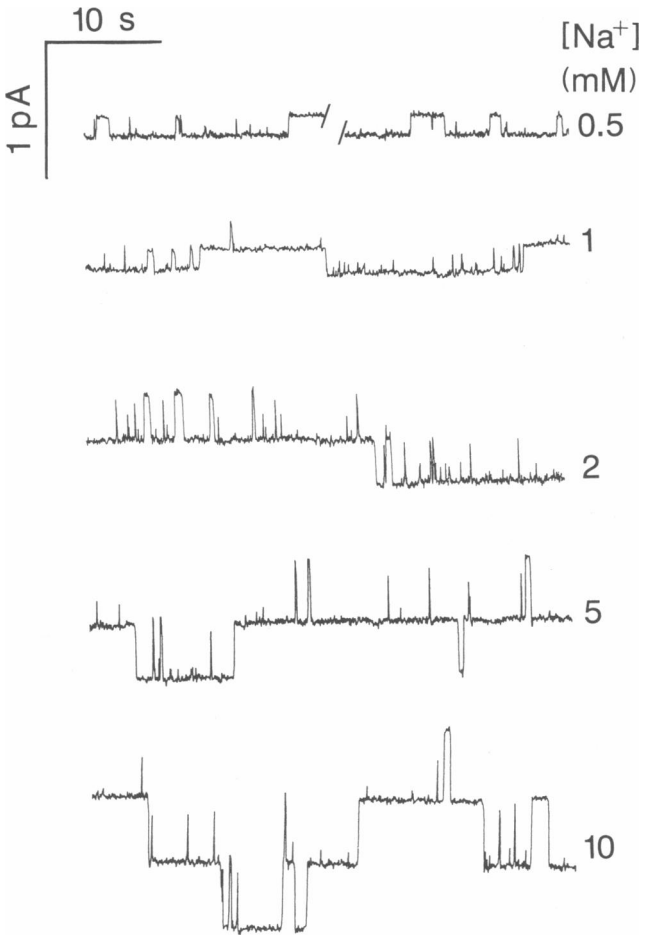

FIGURE 1 Current records of BTX-modified Na^+ channels from rat skeletal muscle at low Na^+ concentrations. Na^+ channel currents were recorded from planar bilayers in the presence of symmetrical solutions containing 0.5, 1, 2, 5, or 10 mM Na^+ as described in Methods. The applied voltage was −50 mV for the *top* record at 0.5 mM Na^+ and −40 mV for the *lower four* records at 1–10 mM Na^+. Channel opening is downward.

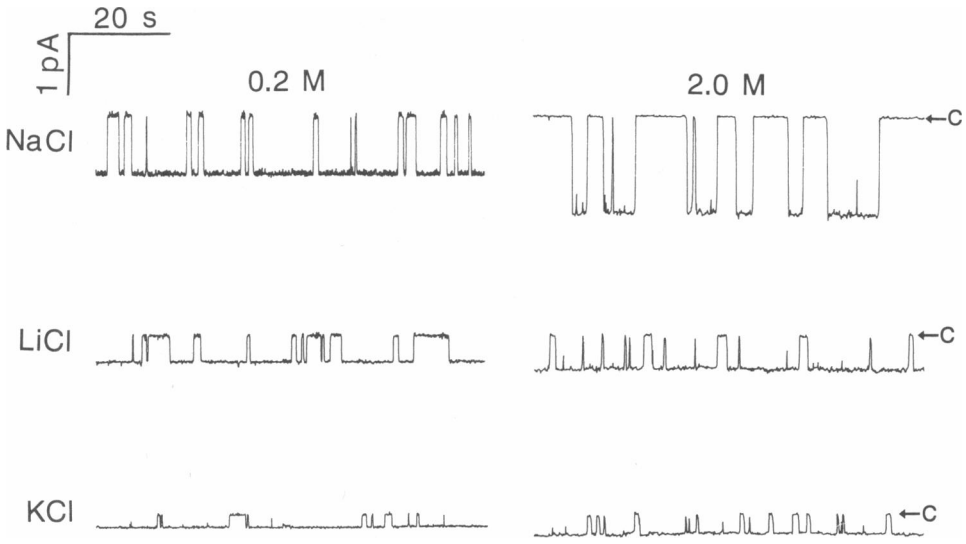

FIGURE 2 Comparison of single-channel currents in the presence of various permeat ions. Na^+ channel currents were recorded in the presence of symmetrical solutions containing either 0.2 M NaCl, LiCl, or KCl (*left*) or 2.0 M NaCl, LiCl, or KCl (*right*). The holding voltage was −50 mV in all cases and openings are downward, as indicated by arrows marking the closed (*c*) current level. Discrete blocking events are due to the presence of 20 nM (*left* records) or 200 nM (*right* records) decarbamoylsaxitoxin on the external side of the channel.

closed or blocked current level. As described previously for BTX-modified Na^+ channels from a variety of sources, the unitary current is exquisitely dependent on the species and concentration of alkali monovalent cations (Hartshorne et al., 1985; Garber and Miller, 1987; Green et al., 1987*a*; Garber, 1988; Behrens et al., 1989; Recio-Pinto et al., 1987).

I-V behavior in the presence of symmetrical Na^+

The data points in Fig. 3 correspond to representative I-V (Fig. 3 *A*) or conductance-voltage (Fig. 3 *B*) relations of rat muscle Na^+ channels recorded at 12 different symmetrical Na^+ concentrations ranging from 0.5 to 2,006 mM (Fig. 3 *A*) and 3,006 mM (Fig. 3 *B*). Close scrutiny of the data suggests that individual I-V relations are curvilinear although the curvature is slight. (Continuous curves are drawn to a theoretical model, as discussed later.) The linearity and symmetry of the I-V relations can be more critically evaluated in the format of Fig. 3 *B*, which plots the measured chord conductance at positive and negative voltages as a function of the absolute value of applied voltage at several different Na^+ concentrations. Despite the rather low voltage range of our data (±80 mV), the close correspondence of positive and negative chord conductance is suggestive of an underlying symmetry in the energy profile for Na^+ permeation with respect to voltage. This behavior is indicative of a symmetrical barrier structure (Eisenman and Horn, 1983); i.e., the location and heights of the energy barriers are expected to be symmetrical about the center of the field in order to produce the same absolute Na^+ current at high positive voltage vs. high negative voltage. A simple interpretation of such I-V symmetry at low Na^+ concentration (~1 mM) is that, if net surface charge is present near the inner and outer channel vestibules, it must be at a similar desnity for both vestibules. Otherwise, the side with greater negative surface charge would be expected to show a larger current because of an enhanced local concentration of Na^+ ions (Dani, 1986; Imoto et al., 1988). The chord conductance plots of Fig. 3 *B* also indicate a slight tendency toward superlinearity of the I-V curves at higher voltage, which suggests that the barriers for Na^+ entry are not rate determining, since high entry barriers and low internal barriers have been shown to result in sublinear I-V curves at low concentration (Eisenman et al., 1980; Eisenman and Horn, 1983).

Since the single-channel I-V curves are essentially linear at low voltages, the slope conductance at 0 mV, g_0, was estimated by linear regression of I-V data points in the range of −50 to +50 mV. Average zero-voltage conductance values are plotted vs. Na^+ concentration in both log–log and linear format in Fig. 4. The results indicate that unitary conductance exhibits a biphasic dependence on $[Na^+]$. At low $[Na^+]$, g_0 for the muscle Na^+ channel approaches a linear function of $[Na^+]$, as indicated by comparison with a slope of 1.0 in the log–log plot of Fig. 4 *A*. At $[Na^+]$ in the range of 50 to

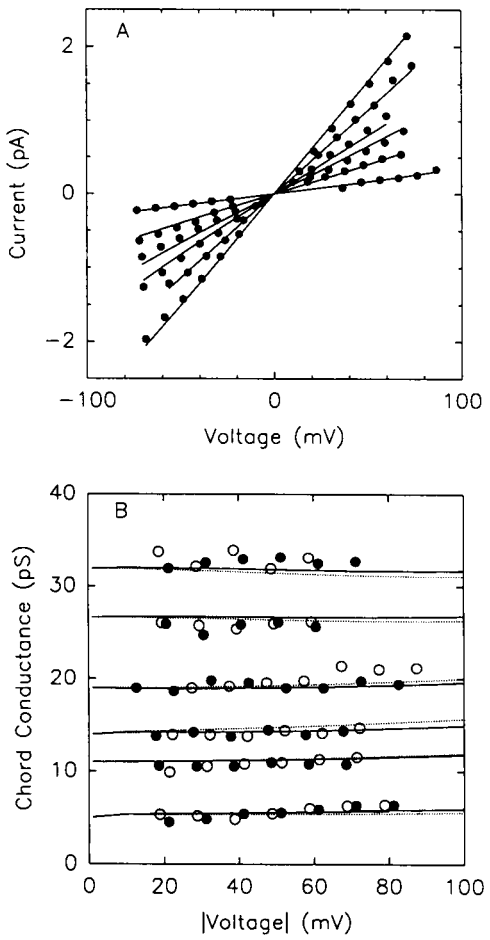

FIGURE 3 Single-channel current–voltage and conductance–voltage behavior of BTX-modified Na^+ channels from rat skeletal muscle at various concentrations of symmetrical Na^+. Data points are experimental current–voltage (*A*) or conductance–voltage (*B*) data from representative bilayers at 12 different Na^+ concentrations. Continuous lines are theoretical curves of the best-fit 3B2S model with parameters for Na^+ listed in Table I. (*A*) Data and curves of increasing slope correspond to the following concentrations of symmetrical Na^+ (mM): 0.5, 2, 10, 56, 506, and 2,006. (*B*) The chord conductance (from 0 mV) is plotted vs. the absolute value of voltage. Open circles and dotted lines correspond to current measurements at negative voltages; closed circles and solid lines correspond to current measurements at positive voltages. Data from low to high conductance values correspond to the following increasing concentrations of symmetrical Na^+ (mM): 1, 5, 20, 206, 1,006, and 3,006.

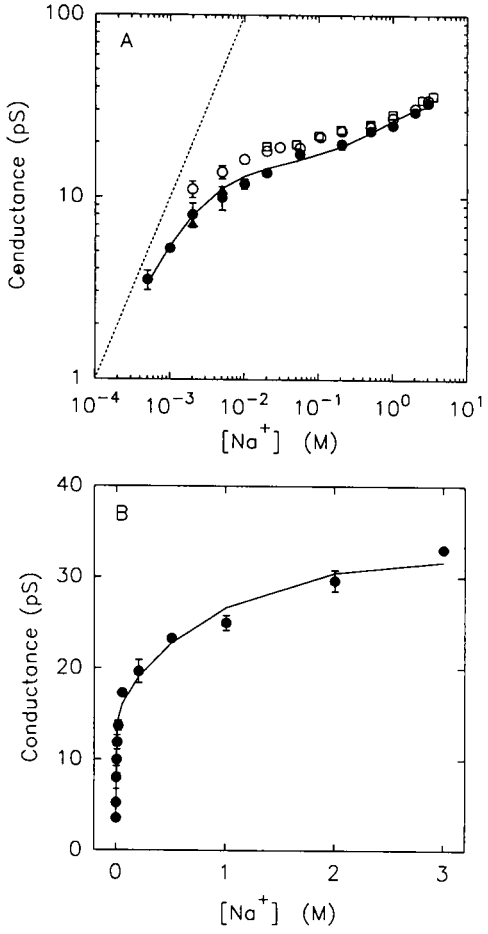

FIGURE 4 Conductance–concentration behavior of BTX-modified Na^+ channels. (*A*) Comparison of three different Na^+ channel subtypes plotted in log–log format. Solid symbols, Na^+ channels from rat skeletal muscle; open circles, Na^+ channels from canine heart; open squares, Na^+ channels from canine brain (data of Green et al., 1987*a*). For rat muscle, solid triangles refer to two experiments in the presence of 0.5 mM Na_4(EDTA) as described in Methods. Dashed line indicates a slope of 1.0. Solid line connects theoretical points for the best-fit 3B2S model with parameters for Na^+ listed in Table 1. (*B*) Same data for rat muscle Na^+ channels is shown in linear format for comparison. Where shown, error bars refer to standard deviations larger than the symbol for data collected from 3–14 bilayers.

500 mM, g_0 appears to saturate, as found previously (Moczydlowski et al., 1984), but higher Na^+ concentrations produce a second rising phase. In the log–log plot of Fig. 4 *A*, this behavior appears as an inflection in the $\log g_0$ vs. $\log [Na^+]$ plot near 100 mM $[Na^+]$. In the linear plot of Fig. 4 *B*, the g_0 vs. $[Na^+]$ behavior appears as a sharp increase at low $[Na^+]$ followed by a more gradual rise to the highest measured conductance value at 3,006 mM Na^+.

From the shape of the curve described by the data of Fig. 4, it is clear that such behavior departs from a simple Michaelis-Menten function. Michaelis-Menten behavior is exhibited by channels with a single binding site or multiple binding sites with single-ion occupancy (Lauger, 1973). Although it is possible to fit the data over a selected low Na^+ concentration range to a Michaelis-Menten function (Moczydlowski et al., 1984; Garber and Miller, 1987), this fit inevitably fails to

describe the data at high Na^+ concentration. For comparison, Fig. 4*A* also shows data from similar experiments with canine heart Na^+ channels (open circles; Ravindran, A., and E. Moczydlowski, unpublished data) and canine brain Na^+ channels (*open squares*; Green et al., 1987*a*). This comparison shows that the cardiac Na^+ channel exhibits behavior similar to that of the muscle channel, except that the heart channel is higher in unitary conductance by ~2 pS. Over the measured concentration range, the conductance data for dog brain appear similar to those of canine heart; however, the brain data have been previously described by a surface charge model that predicts a limiting conductance plateau at a low Na^+ concentration (Green et al., 1987*a*). At concentrations <20 mM Na^+, the heart Na^+ channel exhibits a gradual decrease in conductance but does not reach a definite conductance plateau at 2 mM Na^+ (Fig. 4*A*).

A possible artifact that could potentially interfere with the detection of a surface charge effect in such systems is the presence of contaminating divalent cations (Apell et al., 1979). If there are clusters of negative surface charges in the channel vestibule that happen to bind divalent cations such as Ca^{2+}, then low levels of such divalent cations might obscure the effect of negative surface charges on Na^+ permeation by binding at low ionic strength. In our standard protocol for these experiments, we attempted to eliminate this possible artifact by including low concentrations (0.05–0.2 mM) of EDTA as a chelating agent for divalent cations (see Methods). As an additional control, we also repeated unitary I-V measurements for the rat muscle channel at 2 and 5 mM Na^+ with alternative solutions containing fivefold higher EDTA (0.5 instead of 0.1 mM) than usual. If contaminating divalent cations had contributed to the depression of conductance values at low ionic strength, then we would have expected to observe a larger conductance in the presence of 0.5 mM EDTA. As shown by the two data points represented by filled triangles in Fig. 4*A*, the fivefold increase in EDTA did not significantly affect the unitary conductance. This result eliminates the possibility that the observed conductance decrease at low Na^+ concentration is an artifact related to the presence of divalent cations.

In previous studies of BTX-modified Na^+ channels, several authors have attempted to explain the shape of g_0 vs. [Na^+] data on the basis of models incorporating negative surface charge at both entrances of the channel (Green et al., 1987*a*; Cai and Jordan, 1990; Correa et al., 1991). In the absence of detailed knowledge of the shape of channel vestibules and the exact distribution of net charge at the entrances, it is convenient to assume a planar distribution of smeared negative charge according to the Gouy-Chapman theory of ion concentrations near the surface of an infinite plane (Green and Andersen, 1991). However, this particular theory of planar negative surface charge predicts finite limiting values of surface cation concentrations in the limit of low ionic strength, which results in a predicted conductance plateau in the limit of zero [Na^+] (Green et al., 1987*a*; Correa et al., 1991). From the data of Fig. 4*A*, there is no evidence of such a plateau conductance for the rat muscle channel at low ionic strength. Therefore, if negative surface charge functions in the enhancement of Na^+ conduction, The Gouy-Chapman model does not provide a good analogy of the surface charge distribution in our case. Cai and Jordan (1990) have shown that a more realistic model of vestibule surface charge, in which the negative charge is specifically localized to the channel entrance, does predict an enhanced conductance that approaches zero in the limit of low [Na^+]. Thus, the rat muscle Na^+ channel may best be described by permeation models that incorporate such a Cai-Jordan description of vestibule surface charge. But in view of the fact that the structure of the Na^+ channel and its surface charge topology is currently unknown, we have decided to explore the predictions of a model that does not incorporate surface charge.

Since Hille and Schwarz (1978) previously showed that permeation models incorporating multiple occupancy and ion–ion repulsion can produce biphasic g_0 vs. [Na^+] behavior similar to that observed for the rat muscle channel (see also Hille, 1984, p. 267), we investigated the applicability of an Eyring model for the simplest multi-ion channel, a 3B2S double-occupancy model as described in Methods. Simultaneous nonlinear least-square fitting of all the data points shown in Fig. 3 yielded a set of well-defined energy parameters for Na^+ (Table 1) that closely simulates the I-V behavior over the tested range of Na^+ concentration. Comparison of the behavior predicted by the 3B2S model with the actual data points is indicated by solid or dotted lines connecting theoretical points in Figs. 3 and 4. The best-fit barrier profile for Na^+ shown in Fig. 9 displays a symmetric profile with peaks uniformly close to 3.3 RT units and both wells at −9.6 RT. The symmetrical shape of the best-fit energy profile with respect to the central barrier is consistent with the symmetrical I-V curves. The final distance or *D* parameters (see Fig. 9 for definitions) used to fit the Na^+ data were arrived at by constraining the location of the middle barrier at an electrical distance of 0.5 and imposing a symmetry constraint about this peak such that *D1* = *D6*, *D2* = *D5*, and *D3* = *D4*. With these restrictions, the fitting routine yielded a rather uniform voltage dependence of the various transitions as indicated by best-fit D values near ~0.167 or ⅙. However, in our experience, the fitting routine can produce fits nearly as good as those in Fig. 3

TABLE 1 **Best fit energy parameters of the 3B2S double-occupancy model for Na^+, Li^+, and K^+**

Parameter	Na^+	Li^+	K^+
G1	3.29 ± 0.06	3.54 ± 0.07	1.00
G2	3.22 ± 0.04	3.43 ± 0.05	5.47 ± 0.13
G3	3.50 ± 0.05	3.66 ± 0.06	5.93 ± 0.15
U1	−9.61 ± 0.04	−10.40 ± 0.04	−10.23 ± 0.03
U2	−9.64 ± 0.04	−10.37 ± 0.04	−8.03 ± 0.15
A1	2.16 ± 0.03	2.16	2.16
A2		2.16	2.16
A12		2.16	2.16
SUMSQ	0.358	1.05	0.562

Best-fit values of 3B2S parameters in RT units are listed for I-V data in the presence of Na^+ alone, Na^+ plus Li^+, and Na^+ plus K^+. Standard deviations derived from the fitting procedure are given for parameters that were free to vary. Values that are shown with no uncertainty were held constant. The following distance parameters were held constant in the fitting routine as described in the text: $D1 = D2 = D5 = D6 = 0.175$ and $D3 = D4 = 0.15$. SUMSQ is the weighted sum of squared differences of experimental and theoretical data minimized by the fitting routine (Alvarez et al., 1991). The solution reference state is 55.5 M.

with various other values of the distance parameters, as long as distance symmetry about the middle peak is preserved. For the final fits presented in this paper, we chose fixed distance parameters close to a uniform voltage dependence for each transition, with the *D3* and *D4* electrical distances (0.15) only slightly smaller than the other distances (0.175).

As elaborated in the Discussion, ion–ion repulsion is the critical feature of the double-occupancy 3B2S model that produces the distinctive biphasic dependence on $[Na^+]$ seen in Fig. 4*A*. In our model, this repulsion is simulated by an *A1* energy parameter that raises the energy of peaks and wells adjacent to an occupied well by a factor, A/d, that varies inversely with distance to mimic a coulombic interaction. The best-fit value of the *A1* parameter that we obtained for Na^+ ($A1 = 2.16 \pm 0.03$ RT) effectively lowers the affinity of Na^+ binding to a singly occupied channel by a factor of ~1,000. Thus, if our well depth energies are converted to dissociation binding constants (K_d) for Na^+ using the more conventional 1.0 M solution reference state, then Na^+ binding to an unoccupied channel has a K_d of 3.7 mM and Na^+ binding to a singly occupied channel has a K_d of 4,900 mM.

I-V behavior in symmetrical mixtures of Na^+ and Li^+

The "anomalous mole-fraction effect" is a phenomenon that is widely considered to be diagnostic of a multi-ion channel (Hille, 1984, p. 269). This effect refers to the observation of a minimum in unitary conductance as a function of the mole fraction of two permeant test ions held at a constant total ionic strength (e.g., Neher, 1975; Eisenman et al., 1977). Figs. 5 and 6 summarize the results of an experiment designed to detect such behav-

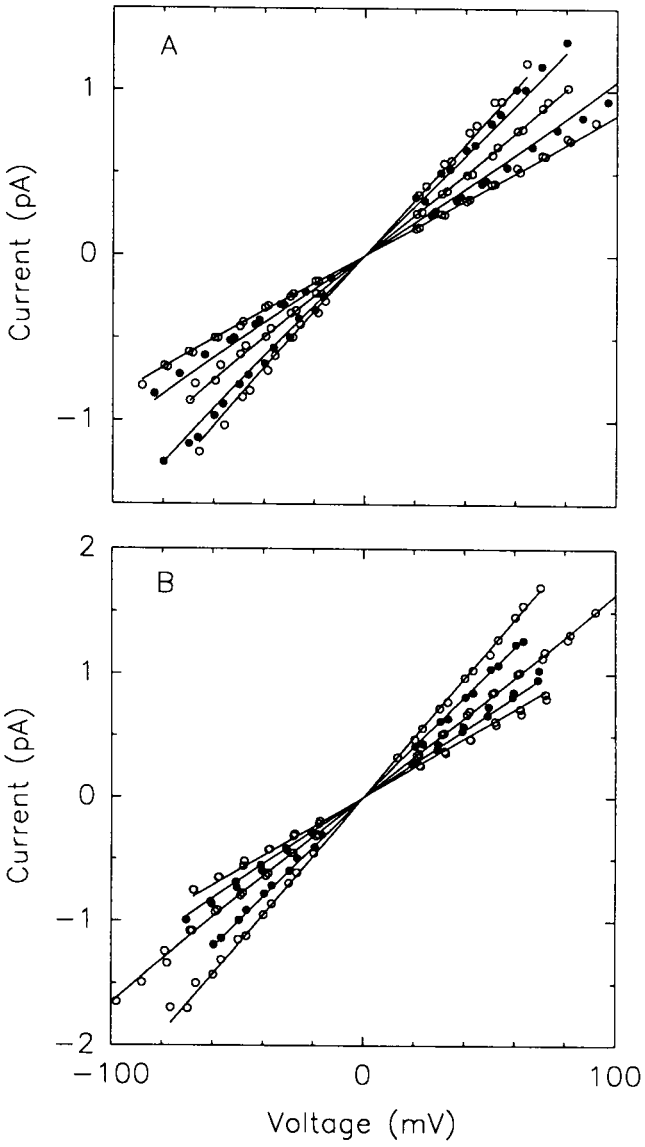

FIGURE 5 Single-channel current–voltage behavior of BTX-modified Na^+ channels in symmetrical mixtures of Na^+ and Li^+ at constant ionic strength. (*A*) Total ionic strength: 206 mM. Curves of increasing slope correspond to the following Na^+/Li^+ mixtures (mM): 6/200, 56/150, 106/100, 156/50, and 181/25. (*B*) Total ionic strength: 2,006 mM. Curves of increasing slope refer to Na^+/Li^+ mixtures (mM): 6/2,000, 506/1,500, 1,006/1,000, 1,506/500, 1,756/250. Solid lines correspond to the theoretical behavior of the best-fit 3B2S model with parameters for Na^+ and Li^+ listed in Table 1. Good fits were also obtained for I-V data at 31 Na^+/175 Li^+ and 256 Na^+/1,750 Li^+ but are not shown to ease crowding of the data.

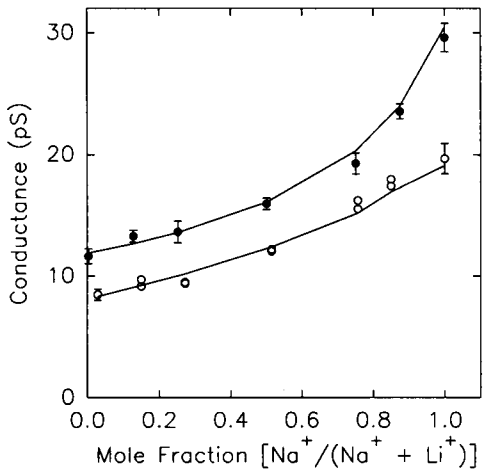

FIGURE 6 Conductance at 0 mV of BTX-modified Na^+ channels from rat muscle as a function of the activity mole fraction of Na^+ in Na^+–Li^+ symmetrical mixtures. Open circles, 206 mM total ionic strength; closed circles, 2,006 mM total ionic strength. Solid lines refer to predictions of the 3B3S model with parameters for Na^+ and Li^+ in Table 1.

ior for mixtures of Na^+ and Li^+ at 0.2 and 2.0 M total salt concentration. The results indicate that I-V curves in mixtures of Na^+ plus Li^+ closely approximate ohmic behavior under the tested conditions (Fig. 5). Intuitively, such behavior would be expected in a situation where both permeant ions display symmetric energy profiles.

To apply the 3B2S model to the Na^+/Li^+ data, we fitted the I-V data in Fig. 5 to the case of net current produced by two permeant species present on both sides of the channel. In the fitting procedure, the energy parameters for Na^+ and the distance parameters were fixed to those previously determined for the case of pure Na^+. All of the energy parameters for Li^+ were initially allowed to vary. This strategy resulted in a best-fit barrier profile for Li^+ that is rather similar to that for Na^+, with an increase in peak heights of ~0.2 RT units and a decrease in well depths of ~0.8 RT units for Li^+ compared with Na^+ (Table I, Fig. 9). The best-fit ion–ion interaction energies (A parameters) for Li^+–Li^+ ($A2$ = 2.16 ± 0.06 RT) and Na^+–Li^+ ($A12$ = 1.91 ± 0.03 RT) were essentially equivalent to $A1$ = 2.16 RT previously found for the Na^+–Na^+ interaction (Table I). In view of the close agreement between the various A's for an unrestricted fit, we fixed all three A parameters to 2.16 RT and refit the I-V data of Fig. 5 with the peak (G) and well (U) energies for Li^+ as the only variables. The fit for the Li^+ energies obtained in this manner was visually indistinguishable from the fit with variable $A2$ and $A12$. When the Na^+–Li^+ mole-fraction data are plotted as zero-voltage conductance vs. the mole fraction of Na^+, the observed behavior was essentially monotonic with no hint of a minimum (Fig. 6). The best-fit 3B2S parameters for Na^+ and Li^+ listed in Table 1 faithfully simulate the observed I-V data and the mole fraction dependence at both 0.2 and 2.0 M total salt concentration as indicated by the solid lines in Figs. 5 and 6.

I-V behavior in symmetrical mixtures of Na^+ and K^+

Results of mole-fraction experiments in the presence of symmetrical Na^+ plus K^+ at 0.2 and 2.0 M total concentration are presented in Figs. 7 and 8. In contrast to the nearly ohmic behavior observed in pure Na^+ or mixtures of Na^+ and Li^+, I-V curves in the presence of Na^+ plus K^+ exhibit a distinctive inward rectification (Fig. 7). This phenomenon is quite similar to the previously described blocking effect of internal K^+ on BTX-modified Na^+ currents (Garber and Miller, 1987; Garber, 1988). The mole-fraction dependence of unitary current at −50 and +50 mV is plotted separately in Fig. 8 A and B. At both 0.2 and 2.0 M total concentration of Na^+ plus K^+, the current follows a monotonic dependence on the Na^+ mole fraction without any suggestion of a minimum. However, these data follow a concave downward function at −50 mV (Fig. 8 A) and a concave upward function at +50 mV (Fig. 8 B).

As in the case of Li^+, we initially attempted to fit the results in mixtures of Na^+ and K^+ to the 3B2S model by fixing the energy parameters for Na^+ and the distance parameters to the best-fit values previously determined for the pure Na^+ case and allowing all of the energy parameters for K^+ to vary. With this approach, the fitting routine converged but did not produce excellent fits as judged by rather large standard errors for several of the energy parameters for K^+. In particular, the height of the inner barrier, $G1$ (0.92 ± 1.1 RT), and the K^+–K^+ interaction energy, $A2$ (0.96 ± 0.52 RT), were poorly determined, as judged by rather large standard errors. For the fit shown in Figs. 7 and 8, we constrained the $G1$ parameter to 1.0 RT and also constrained both the $A2$ and $A12$ interaction energies to 2.16 RT, similar to the values determined for Na^+ and Li^+. A constant value for the A parameters for all of the ions is the most physically meaningful choice if we assume that ion–ion interactions are due to electrostatic repulsion between ions of the same valence and distance of separation. With these constraints, the fitting procedure resulted in well-defined values for the other K^+ energy parameters, as indicated by low standard errors (Table 1). The barrier profile for K^+ corresponding to this fit (Fig. 9) is asymmetric, as would be predicted from the rectifying I-V curves in the presence of K^+. The inward rectifica-

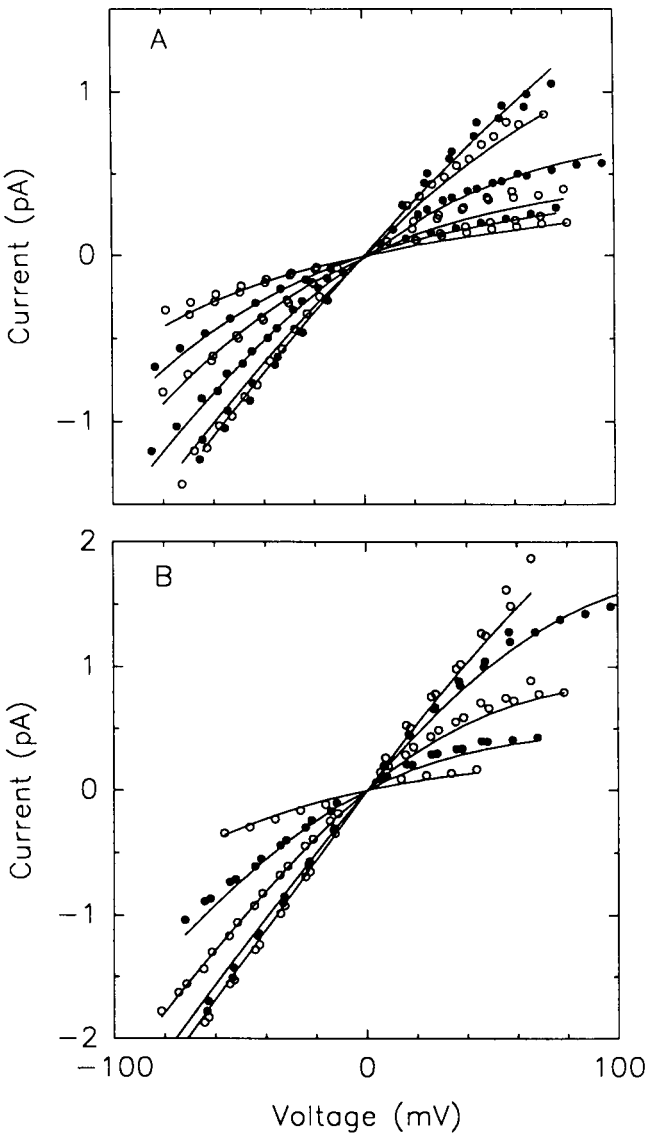

FIGURE 7 Single-channel current-voltage behavior of BTX-modified Na^+ channels in symmetrical mixtures of Na^+ and K^+ at constant ionic strength. (*A*) Total ionic strength: 206 mM. Curves of increasing slope correspond to the following Na^+/K^+ mixtures (mM): 6/200, 31/175, 56/150, 106/100, 156/150, and 181/25. (*B*) Total ionic strength: 2,006 mM. Curves of increasing slope refer to Na^+/K^+ mixtures (mM): 6/2,000, 506/1,500, 1,006/1,000, 1,506/500, and 1,756/250. Solid lines connect theoretical points predicted by the best-fit 3B2S model with parameters for Na^+ and K^+ listed in Table 1.

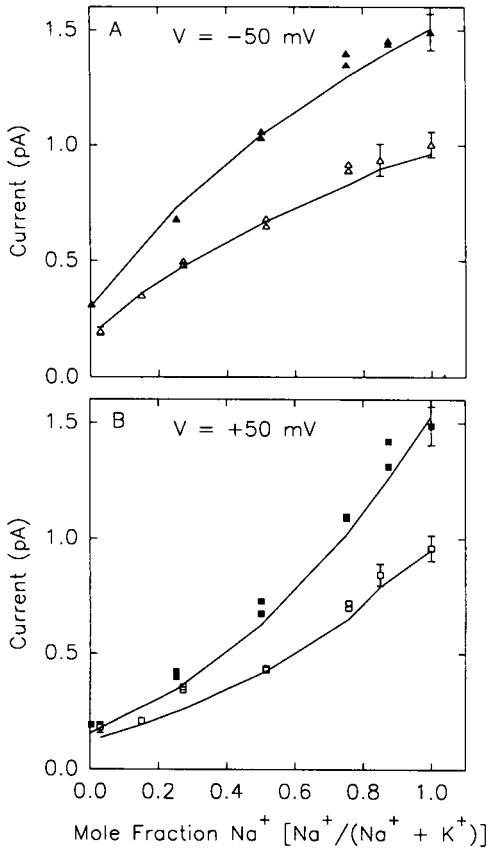

FIGURE 8 Unitary current of BTX-modified Na^+ channels from rat muscle as a function of the activity mole fraction of Na^+ in symmetrical mixtures of Na^+ and K^+. (*A*) Current values at −50 mV. (*B*) Current values at 50 mV. Open symbols, 206 mM total ionic strength; closed symbols, 2,006 mM total ionic strength. Solid lines connect theoretical points predicted by the best-fit 3B2S model with parameters for Na^+ and K^+ listed in Table 1.

tion appears to be the result of a deeper inner vs. outer well for K^+ and a higher rate-limiting inner barrier for outward vs. inward K^+ movement. This 3B2S energy profile for K^+ provides a relatively good simulation of the I-V and mole-fraction behavior in the presence of Na^+ plus K^+, as indicated by the solid line curves in Figs. 7 and 8.

Although the mole-fraction data for Na^+–Li^+ and Na^+–K^+ mixtures do not display an anomalous minimum that might be accepted as virtual proof of multi-ion conduction, these results are nevertheless instructive. The ability of the 3B2S double-occupancy model to simulate monotonic behavior in the mole-fraction dependence of ion mixtures is a reminder that the classic anomalous mole fraction effect is only predicted by certain pairs of barrier profiles in Eyring models of permeation. In the 3B2S models explored by Hille and Schwarz (1978), anomalous minima were predicted when the energy profile for at least one of the ions has high barriers at both ends of the channel (Hille, 1984, p. 268). This special requirement for the effect is apparently not exhibited by Na^+, Li^+, and K^+ in the BTX-modified Na^+ channel that we have studied.

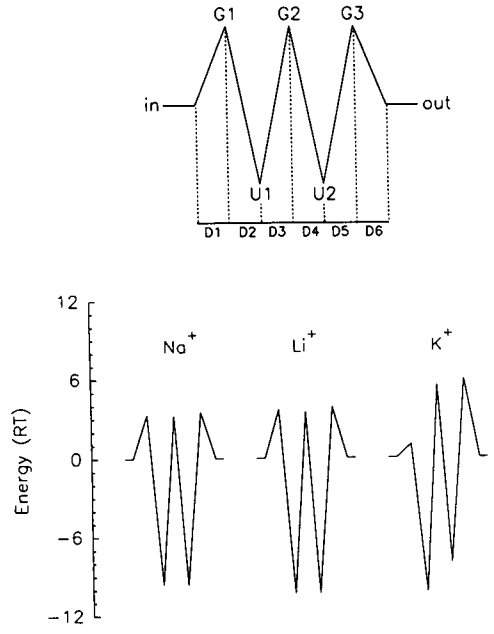

FIGURE 9 Best-fit energy barrier profiles for Na^+, Li^+, and K^+ that predict permeation through BTX-modified Na^+ channels from rat muscle. The *upper* diagram defines the adjustable 3B2S model parameters of peak energies (*G1*, *G2*, and *G3*), well energies (*U1* and *U2*), and distances (*D1–D6*) with respect to the inner and outer solutions. The *lower* diagram shows best-fit energy profiles of the unoccupied channel at 0 mV for Na^+, Li^+, and K^+ drawn according to parameter values listed in Table 1 and the distance parameters: $D1 = D2 = D5 = D6 = 0.175$ and $D3 = D4 = 0.15$.

DISCUSSION

This paper documents three observations that are relevant to the mechanism of ion permeation through BTX-modified Na^+ channels of rat skeletal muscle: (*a*). The dependence of unitary conductance on symmetrical $[Na^+]$ does not obey a Michaelis-Menten function over the range of 0.5 to 3,000 mM Na^+. (*b*) The unitary conductance appears to approach zero in the limit of low $[Na^+]$. (*c*) The unitary conductance exhibits a monotonic dependence on the Na^+ mole fraction in constant ionic strength mixtures of Na–Li and Na–K.

On the basis of previous evidence that Na^+ channels can exhibit various features of multiple-ion occupancy (Begenisich, 1987), we have attempted to interpret our results according to a basic permeation model for a multi-ion channel. Our modeling results serve to reconcile the dual personality of Na^+ channel permeation, which can display characteristic features of single- or multi-ion conduction depending on the conditions of assay. Assuming that surface charge effects may be neglected, the observed dependence of unitary conductance on Na^+ concentration cannot be explained by a channel that can only accommodate one ion at a time. When this dependence is examined over a 6,000-fold concentration range (Fig. 4), we do not observe saturating Michaelis-Menten behavior expected of single-occupancy pores. Instead, we find a more complex concentration dependence, which can be adequately represented by a two-site, double-occupancy model. This finding emphasizes the importance of studying the widest possible range of permeation concentration in such experiments. An earlier study of this channel (Moczydlowski et al, 1984) was misled in favor of single-site behavior by limiting the investigation to a smaller 100-fold range of Na^+ concentration. Indeed, in a textbook chapter that outlines the properties of multi-ion channels, Hille (1984, p. 266) cautions: "In practical experiments, limited to concentration changes of only one or two orders of magnitude, the conductance (of multi-ion channels) might appear to obey the predictions of independence or of simple one-ion saturation."

An appreciation of the compatibility of our results with a multi-ion pore can be gained by comparing the data in Fig. 4 of this paper with the generalized theoretical behavior of a 3B2S double-occupancy model as summarized in Fig. 3 of Hille and Schwarz (1978). For a two-site channel with no repulsion between ions in the doubly occupied state, the conductance is expected to be a linear function of $[Na^+]$ at the low concentration limit. At higher $[Na^+]$ the predicted conductance–concentration relation rises to a maximum and actually decreases in the high concentration limit, when the net flux is inhibited due to an increasing probability of the doubly occupied state. In the case of repulsion between two ions in the channel, barrier profiles other than those with a high central barrier predict behavior similar to that of our Fig. 4, i.e., a biphasic increase that is partly due to an enhanced rate of exit from the channel in the doubly occupied state (Hille and Schwarz, 1978). The 3B2S model with repulsion also predicts a phase of decreasing conductance in the high $[Na^+]$ limit. For our particular barrier profile for Na^+, a theoretical conductance maximum of 32.0 pS is predicted at a Na^+ concentration of 3.2 M. This predicted maximum occurs just above our range of observation at 3.0 M NaCl and is difficult to verify experimentally because of the insolubility limit.

Considering the structural and functional complexity of Na^+ channels in comparison to the 3B2S model, it is remarkable that the set of three energy profiles in Fig. 9 can simulate the whole concentration range of data that we have gathered for Na^+, Li^+, and K^+. To further evaluate the predictive ability of the 3B2S model, we can compare the theoretical behavior of this model to the results of Garber and Miller (1987) and Garber (1988), who reported complementary permeation data on the

TABLE 2 **Comparison of experimental bi-ionic reversal potentials with predictions of the 3B2S double-occupancy model**

	$[Li^+]_{in}/[Na^+]_{out}$		$[Li^+]_{out}/[Na^+]_{in}$	
Concentration	Exp	3B2S	Exp	3B2S
mM	*mV*	*mV*	*mV*	*mV*
57	2.4	4.0	−4 ± 4	−4.0
207	—	1.7	−3 ± 2	−1.7
507	2.4	−0.8	−3 ± 3	0.8
	$[K^+]_{in}/[Na^+]_{out}$		$[K^+]_{out}/[Na^+]_{in}$	
mM	*mV*	*mV*	*mV*	*mV*
57	30	40.5	−53 ± 5	−57.3
207	35 ± 5	40.6	−57 ± 4	−57.5
507	38	40.6	−51 ± 4	−57.6

Experimental (Exp) reversal potentials are results of Garber and Miller (1987) and Garber (1988) for BTX-modified Na^+ channels from rat skeletal muscle measured under various bi-ionic conditions as indicated. Theoretical (3B2S) reversal potentials are predicted by the 3B2S double-occupancy model of this paper using the energy parameters of Table 1. BTX, batrachotoxin.

same channel. A measure of laboratory-to-laboratory consistency can be obtained by comparing absolute conductance values predicted by our 3B2S barrier profiles with conductance values reported by Garber and Miller (1987) for defined symmetrical conditions of 500 mM Na^+, Li^+, or K^+. For 500 mM symmetrical Na^+, Garber and Miller (1987) reported a zero-voltage conductance of 21 ± 2 pS compared with a prediction of 23.0 pS for our model. A similar comparison for 500 mM Li^+ is 9 ± 2 pS (Garber and Miller, 1987) vs. 10.1 pS (3B2S model). In the range of −100 to 0 mV, Garber and Miller (1987) reported a slope conductance of 5.7 ± 0.5 pS for 500 mM K^+ vs. 5.9 pS (3B2S model). Thus, this particular test is very successful with only 10% disparity between experiment and theory. Considering that none of our fits included I-V data for conditions of 500 mM Li^+ and 500 mM K^+, this agreement is reassuring.

A second, more stringent test of the 3B2S model can be made by comparing experimental reversal potentials (V_{rev}) measured by Garber (1988) under bi-ionic conditions with the analogous predictions generated from our barrier profiles. Results of this comparison are summarized in Table 2 for four different bi-ionic conditions studied by Garber (1988): $[Li^+]_{in}/[Na^+]_{out}$, $[Li^+]_{out}/[Na^+]_{in}$, $[K^+]_{in}/[Na^+]_{out}$, and $[K^+]_{out}/[Na^+]_{in}$. This comparison also shows good agreement between experiment and the 3B2S model. In the case of bi-ionic conditions of Na^+ vs. Li^+, Garber (1988) reported permeability ratios (P) close to 1.0 for either orientation, i.e., V_{rev} values close to zero with no significant concentration dependence in the range of 57 to 506 mM. The predicted V_{rev} values for our model are with 2 mV of the experimental values, which is close to the error of such measurements. It is also worth noting that Garber (1988) was unable to find a set of barrier profiles for a 4B3S single-occupancy model that predicted both the lower conductance of Li^+ vs. Na^+ and P_{Li}/P_{Na} ratios near 1.0. For single-ion channels, permeability ratios are known to depend only on the difference in peak heights between the energy profiles of two permeant species, whereas, for multi-ion channels, permeability ratios are a function of both the difference in peak heights and well depths (Hille, 1984). Thus, the multi-ion model of permeation is much more flexible in accounting for observed differences in conductance and V_{rev}. In the case of bi-ionic V_{rev} measurements for the Na^+-vs.-K^+ comparison, the agreement between experiment and the 3B2S model is also quite good, except in the case of $[K^+]_{in}/[Na^+]_{out}$ at 57 mM concentration, where there is a 10-mV discrepancy (Table 2). Of particular note in Table 2 is the successful prediction of the orientation-dependent V_{rev}s, which correspond to values of $P_K/P_{Na} \simeq 0.12$ for $[K^+]_{out}/[Na^+]_{in}$ and 0.23–0.30 for $[K^+]_{in}/[Na^+]_{out}$. The agreement between experiment and the 3B2S model is striking, considering that the present barrier profiles for K^+ were obtained by fitting I-V curves obtained with symmetrical mixtures of Na^+ plus K^+ and not under bi-ionic conditions of the V_{rev} measurements.

A third test of the 3B2S model can be made by comparing the voltage dependence of K^+ block that is observed when increasing concentrations of symmetrical K^+ are added to a BTX-modified Na^+ channel in the presence of fixed symmetrical Na^+. When this experiment is performed by addition of increasing K^+ to a control in the presence of 57 mM symmetrical Na^+, an effective valence ($z\delta$) of −0.7 to −0.8 for the K^+ blocking reaction was reported (Garber and Miller, 1987; Garber, 1988), using an analysis based on the Woodhull (1973) description of voltage-dependent block. However, when the K^+ blocking experiment of Fig. 7*A* of Garber (1988) was simulated by the present 3B2S model, we obtained a much lower apparent voltage dependence of block; i.e., $z\delta = -0.28$. Thus, the present 3B2S model fails to accurately predict the steep voltage dependence of K^+ block. This deficiency is also apparent in the fits of Fig. 7, where it can be seen that the theoretical curves do not quite exhibit the same degree of curvature shown by the inwardly rectifying experimental I-V data in the presence of mixtures of Na^+ plus K^+. Therefore, this test reveals an inconsistency of the present 3B2S model when it is rigorously compared with actual observations. To amend the present permeation model to more accurately predict the voltage dependence of K^+ block, we would probably have to make the model more

complex by introducing a third ion-binding site, resulting in a 4B3S triple-occupancy model.

Direct comparison of Eyring permeation models for BTX-modified Na^+ channels with those proposed for normal Na^+ channels is not possible because it is known that BTX alters both permeability ratios and the absolute conductance of various permeant ions (Huang et al., 1982; Shenkel et al., 1989; Correa et al., 1991). However, it is important to note that the same basic observations on normal squid axon Na^+ currents that led Begenisich and Cahalan (1980*a*) to first propose a multi-ion model for the Na^+ channel are also inherent properties of the present 3B2S model derived for a BTX-modified Na^+ channel. When Cahalan and Begenisich (1976) varied K^+ inside squid axon at constant 400 mM Na^+ outside, they observed an 40-mV change in reversal potential per 10-fold change in internal K^+ activity. This 40-mV/decade shift in V_{rev} was much less than the theoretical value of 56 mV/decade that would be predicted by Nernst-Planck electrodiffusion theory or by a one-ion Eyring barrier model of permeation at the temperature (15°C) of their experiments. Our present 3B2S model predicts ~49 mV/decade, which is not quite as shallow as that observed for the squid axon but is nevertheless consistent with this classic deviation from Nernstian behavior that can be exhibited by multi-ion channels. It is important to recognize that this particular test of multi-ion behavior depends on the barrier profiles and conditions of assay. Table 2 shows that our 3B2S model does not predict concentration-dependent permeability ratios when bi-ionic reversal potentials are measured over an ~10-fold concentration range of symmetrically varied Na^+ and K^+. Yet this hallmark of multi-ion permeation is observed for the bi-ionic condition of fixed $[Na^+]_{out}$ and varied $[K^+]_{in}$ that was originally discovered in invertebrate axons (Chandler and Meves, 1965; Cahalan and Begenisich, 1976; Ebert and Goldman, 1976). Therefore, just as for the anomalous mole-fraction effect, the absence of concentration-dependent permeability ratios under one set of conditions does not immediately rule out multi-ion occupancy.

Another feature of the BTX-modified Na^+ channel from rat muscle that is qualitatively consistent with previous squid axon experiments is the inward rectification of instantaneous I-V curves observed under conditions where Na^+ is the primary external permeant species outside the channel and K^+ is the primary internal species (Fig. 7 of Begenisich and Cahalan, 1980*b*). To model this behavior for squid axon Na^+ currents, Begenisich and Cahalan (1980*b*) used a nearly symmetrical 3B2S barrier profile for Na^+ and a more asymmetrical profile for K^+ with a deeper internal well and a high rate-limiting barrier for movement of K^+ from the external site to the internal site. This distinctive property of Na^+ channels, depicted by the energy barrier profiles of Fig. 9, poses an important question that will be an enticing goal of future molecular studies of the channel: what is the structural feature of the pore that enables Na^+ and Li^+ to move with roughly equivalent rates in either direction but imposes a barrier that selectively inhibits the movement of K^+ in the outward direction?

Fig. 4 *A* shows a comparison of our data on the g_0 vs. $[Na^+]$ dependence of BTX-modified Na^+ channels from rat muscle and dog heart with data from a similar experiment reported by Green et al. (1987*a*) for Na^+ channels from dog brain. By assuming a single-occupancy model of Na^+ permeation, Green et al. (1987*a*) were able to convincingly model their results with a Michaelis-Menten dependence on local Na^+ concentration in the vicinity of the channel's vestibule, where $[Na^+]_{local}$ is given by the Gouy-Chapman theory of planar surface charge. As described above, this particular theory of ion permeation has the distinguishing feature of a plateau region of $[Na^+]_{local}$ in the low concentration limit, which gives rise to a predicted conductance plateau in the limit of low $[Na^+]$ (Green et al. 1987*a*).

Comparison of the data for the three different Na^+ channels in Fig. 4 *A* shows that an unambiguous detection of a low-salt conductance plateau depends critically on the availability of sufficient data in the low-salt region. For example, if one were to compare only the dog brain and dog heart conductance data in the region above 20 mM Na^+, one might conclude that both channels display a similar low-salt plateau indicative of a substantial negative surface charge. However, by making additional measurements of the dog heart Na^+ channel down to 2 mM Na^+, we observed that the unitary conductance continued to decrease. Despite the importance of such low-salt measurements, technical limitations can sometimes prevent them, as in the case of dog brain Na^+ channels, which exhibit "flickery" conductance behavior at low $[Na^+]$ (Green et al., 1987*a*).

Our modeling results are a reminder that a plateau-like region or an inflection in plots of $\log(g_0)$ vs. $\log[Na^+]$ is also a characteristic feature of multi-ion permeation models that incorporate ion–ion repulsion between adjacent sites (Hille and Schwarz, 1978). Thus, the observation of a tendency of conductance measurements to plateau at low $[Na^+]$ can suggest two very different interpretations: (*a*) surface charge at the mouth of the channel that mimics the effect of the planar charge distribution of Gouy-Chapman theory or (*b*) a multi-ion channel with widely separated ion-binding affinities to successively occupied sites.

Although our rat muscle data can be adequately fit by a multi-ion pore model without surface charge, it is important to recognize that our results do not rule out a

possible influence of negative surface charge on the conduction process. More realistic geometrical models of negative surface charge situated within a funnel-shaped vestibule of a cation channel do predict conductance–concentration behavior that approaches zero conductance in the low-salt limit, when the electrostatic potential due to the fixed negative charge is computed by the nonlinear Poisson-Boltzmann equation (Dani, 1986; Cai and Jordan, 1990). Such behavior is compatible with Fig. 4 of this paper. In this modeling study, we have initially avoided an attempt to incorporate negative surface charge in the 3B2S permeation model in order to ascertain how well this multi-ion barrier model performs on its own. To a first approximation, the results indicate that a multi-ion permeation model that excludes surface charge effects is reasonable; however, there is a variety of independent evidence supporting the role of negative surface charges on various functions of the Na^+ channel: gating (e.g., Hahin and Campbell, 1983; Cukierman et al., 1988), toxin and drug binding (e.g., Green et al., 1987*b*; Ravindran and Moczydlowski, 1989; Smith-Maxwell and Begenisich, 1987), and permeation (e.g., Sigworth and Spalding, 1980; Chabala et al., 1986; Worley et al., 1986; Green et al., 1987*a*). In future modeling studies of Na^+ channel permeation, it will be interesting to test and apply more specialized models of negative vestibule charge, such as those proposed by Dani (1986) and Cai and Jordan (1990), that are coupled to energy profiles of multi-ion pores.

We thank Dr. John Daly for the gift of batrachotoxin and Dr. Ramon Latorre for sharing important manuscripts before publication. We thank Dr. David Busath for helpful discussions.

This work was supported by grants from the National Institutes of Health (NIH) (Ar-38796 and HL-38156 to E. Moczydlowski and GM-24749 to G. Eisenmanr) and FONDECYT (1112-1989 to O. Alvarez). H. Kweicinski was supported by a Fogarty International Fellowship from NIH.

Received for publication 20 February 1991 and in final form 23 September 1991.

REFERENCES

Almers, W., and E. W. McCleskey. 1984. Non-selective conductance in calcium channels of frog muscle: calcium selectivity in a single-file pore. *J. Physiol. (Lond.).* 353:585–608.

Alvarez, O., A. Villarroel, and G. Eisenman. 1992. A general procedure to calculate ion currents from energy profiles and energy profiles from ion currents in a multi-barrier multi-site-occupancy channel model. *Methods Enzymol.* Vol. 207. In press.

Apell, H.-J., E. Bamberg, and P. Lauger. 1979. Effects of surface charge on the conductance of the gramicidin channel. *Biochim. Biophys. Acta.* 552:369–378.

Begenisich, T. 1987. Molecular properties of ion permeation through sodium channels. *Annu. Rev. Biophys. Biophys. Chem.* 16:247–263.

Begenisich, T., and D. Busath. 1981. Sodium flux ratio in voltage-clamped squid giant axons. *J. Gen. Physiol.* 77:489–502.

Begenisich. T. B., and M. D. Cahalan. 1980a. Sodium channel permeation in squid axons. I. Reversal potential experiments. *J. Physiol. (Lond.).* 307:217–242.

Begenisich, T. B., and M. D. Cahalan. 1980b. Sodium channel permeation in squid axons. II. Non-independence and current-voltage relations. *J. Physiol. (Lond.).* 307:243–257.

Behrens, M. I., A. Oberhauser, F. Bezanilla, and R. Latorre. 1989. Batrachotoxin-modified sodium channels from squid optic nerve in planar bilayers. Ion conduction and gating properties. *J. Gen. Physiol.* 93:23–41.

Bell, J. E., and C. Miller. 1984. Effects of phospholipid surface charge on ion conduction in the K^+ channel of sarcoplasmic reticulum. *Biophys. J.* 45:279–287.

Busath, D., and T. Begenisich. 1982. Unidirectional sodium and potassium fluxes through the sodium channel of squid giant axons. *Biophys. J.* 40:41–49.

Cahalan, M. D., and W. Almers. 1979. Interactions between quaternary lidocaine, the sodium channel gates and tetrodotoxin. *Biophys. J.* 27:39–56.

Cahalan, M., and T. Begenisich. 1976. Sodium channel selectivity. Dependence on internal permeant ion concentration. *J. Gen. Physiol.* 68:111–125.

Cai, M., and P. C. Jordan. 1990. How does vestibule surface charge affect ion conduction and toxin binding in a sodium channel? *Biophys. J.* 57:883–891.

Cecchi, X., D. Wolff, O. Alvarez, and R. Latorre. 1987. Mechanisms of Cs^+ blockade in a Ca^{2+}-activated K^+ channel from smooth muscle. *Biophys. J.* 52:707–716.

Chabala, L. D., W. N. Green, O. S. Andersen, and C. L. Borders, Jr. 1986. Covalent modification of external carboxyl groups of batrachotoxin-modified canine forebrain sodium channels. *Biophys. J.* 49:40*a* (Abstr.)

Chandler, W. K., and H. Meves. 1965. Voltage clamp experiments on internally perfused giant axons. *J. Physiol. (Lond.)* 180:788–820.

Correa, A. M., R. Latorre, and F. Benzanilla. 1991. Ion permeation in normal and batrachotoxin-modified Na^+ channels in the squid giant axon. *J. Gen. Physiol.* 97:605–625.

Cukierman, S., W. C. Zinkand, R. J. French, and B. K. Krueger. 1988. Effects of membrane surface charge and calcium on the gating of rat brain sodium channels in planar bilayers. *J. Gen. Physiol.* 92:431–447.

Dani, J. A. 1986. Ion-channel entrances influence permeation. Net charge, size, shape, and binding considerations. *Biophys. J.* 49:607–618.

Danko, M., C. Smith-Maxwell, L. McKinney, and T. Bengenisich. 1986. Block of sodium channels by internal mono- and divalent guanidinium analogues. Modulation by sodium ion concentration. *Biophys. J.* 49:509–519.

Ebert, G. A., and L. Goldman. 1976. The permeability of the sodium channel in *Myxicola* to the alkali cations. *J. Gen. Physiol.* 68:327–340.

Eisenman, G., and R. Horn. 1983. Ionic selectivity revisited: the role of kinetic and equilibrium processes in ion permeation through channels. *J. Membr. Biol.* 76:197–225.

Eisenman, G., J. Sandblom, and E. Neher. 1977. Ionic selectivity, saturation, binding, and block in the gramicidin A channel: a preliminary report. In *Metal-Ligand Interactions in Organic Chemistry and Biochemistry.* part 2. B. Pullman and N. Goldblum, editors. D. Reidel Publishing Co., Dordrect, Holland. 1–36.

Eisenman, G., J. Hagglund, J. Sandblom, and B. Enos. 1980. The

current-voltage behavior of ion channels: important features of the energy profile of the gramicidin channel deduced from the conductance-voltage characteristic in the limit of low ion concentration. *Upsala J. Med. Sci.* 85:247–257.

Eisenman, G., R. Latorre, and C. Miller. 1986. Multi-ion conduction and selectivity in the high-conductance Ca^{2+}-activated K^+ channel from skeletal muscle. *Biophys. J.* 50:1025–1034.

Friel, D. D., and R. W. Tsien. 1989. Voltage-gated calcium channels: direct observation of the anomalous mole fraction effect at the single channel level. *Proc. Natl. Acad. Sci. USA* 86:5207–5211.

Garber, S. S. 1988. Symmetry and asymmetry of permeation through toxin-modified Na^+ channels. *Biophys. J.* 54:767–776.

Garber, S. S., and Miller, C. 1987. Single N^+ channels activated by veratridine and batrachotoxin. *J. Gen. Physiol.* 89:459–480.

Green, W. N., and O. S. Andersen. 1991. Surface charges and ion channel function. *Annu. Rev. Physiol.* 53:341–359.

Green, W. N., L. B. Weiss, and O. S. Andersen. 1987a. Batrachotoxin-modified sodium channels in planar lipid bilayers. Ion permeation and block. *J. Gen. Physiol.* 89:841–872.

Green, W. N., L. B. Weiss, and O. S. Andersen. 1987b. Batrachotoxin-modified sodium channels in planar bilayers. Characterization of saxitoxin- and tetrodotoxin-induced channel closures. *J. Gen. Physiol.* 89:873–903.

Guo, X., A. Uehara, A. Ravindran, S. H. Bryant, S. Hall, and E. Moczydlowski. 1987. Kinetic basis for insensitivity to tetrodotoxin and saxitoxin in sodium channels of canine heart and denervated rat skeletal muscle. *Biochemistry.* 26:7546–7556.

Hahin, R., and D. T. Campbell. 1983. Simple shifts in the voltage dependence of sodium channel gating caused by divalent cations. *J. Gen. Physiol.* 82:785–805.

Hartshorne, R. P., B. U. Keller, J. A. Talvenheimo, W. A. Catterall, and M. Montal. 1985. Functional reconstitution of the purified brain sodium channel in planar lipid bilayers. *Proc. Natl. Acad. Sci. USA.* 82:240–244.

Hess, P., and R. W. Tsien. 1984. Mechanism of ion permeation through calcium channels. *Nature (Lond.).* 309:453–456.

Hille, B. 1975. Ionic selectivity, saturation, and block in sodium channels. A four-barrier model. *J. Gen. Physiol.* 66:535–560.

Hille, B. 1984. *Ionic Channels of Excitable Membranes.* Sinauer Associates, Sunderland, MA. 1–274.

Hille, B., and W. Schwarz. 1978. Potassium channels as multi-ion single-file pores. *J. Gen. Physiol.* 72:409–442.

Huang, L. M., N. Moran, and G. Ehrenstein. 1982. Batrachotoxin modifies the gating kinetics of sodium channels in internally perfused neuroblastoma cells. *Proc. Natl. Acad. Sci. USA.* 79:2082–2085.

Imoto, K., C. Busch, B. Sakmann, M. Mishina, I. Konno, J. Nakai, H. Bujo, Y. Mori, K. Fukuda, and S. Numa. 1988. Rings of negatively charged amino acids determine the acetylcholine receptor channel conductance. *Nature (Lond.).* 335:645–648.

Krueger, B. K., J. F. Worley III, and R. J. French. 1983. Single sodium channels from rat brain incorporated into planar lipid bilayers. *Nature (Lond.).* 303:172–175.

Lauger, P. 1973. Ion transport through pores: a rate theory analysis. *Biochim. Biophys. Acta.* 311:423–441.

Moczydlowski, E., S. S. Garber, and C. Miller, 1984. Batrachotoxin-activated Na^+ channels in planar lipid bilayers. Competition of tetrodotoxin block by Na^+. *J. Gen. Physiol.* 84:665–686.

Moczydlowski, E., O. Alvarez, C. Vergara, and R. Latorre. 1985. Effect of phospholipid surface charge on the conductance and gating of a Ca^{2+}-activated K^+ channel in planar lipid bilayers. *J. Membr. Biol.* 83:273–282.

Neher, E. 1975. Ionic specificity of the gramicidin channel and the thallous ion. *Biochim. Biophys. Acta.* 401:540–544.

Nilius, B. 1988. Calcium block of guinea-pig heart sodium channels with and without modification by the piperazinylindole DPI 201-106. *J. Physiol. (Lond.).* 399:537–558.

Ravindran, A., and Moczydlowski, E. 1989. Influence of negative surface charge on toxin binding to canine heart Na channels in planar bilayers. *Biophys. J.* 55:359–365.

Ravindran, A., L. Schild, and E. Moczydlowski. 1991. Divalent cation selectivity for external block of voltage-dependent Na^+ channels prolonged by batrachotoxin. Zn^{2+} induces discrete substates in cardiac Na^+ channels. *J. Gen. Physiol.* 97:89–115.

Recio-Pinto, E., D. S. Duch, S. R. Levinson, and B. W. Urban. 1987. Purified and unpurified sodium channels from eel electroplax in planar lipid bilayers. *J. Gen. Physiol.* 90:375–395.

Sandblom, J., G. Elsenman, and E. Neher. 1977. Ionic selectivity, saturation and block in gramicidin A channels. I. Theory for the electrical properties of ion selective channels having two pairs of binding sites and multiple conductance states. *J. Membr. Biol.* 31:383–417.

Schild, L., and E. Moczydlowski. 1991. Competitive binding interaction between Zn^{2+} and saxitoxin in cardiac Na^+ channels: evidence for a sulfhydryl group in the Zn^{2+}/saxitoxin binding site. *Biophys. J.* 59:523–537.

Shapiro, B. I. 1977. Effects of strychnine on the sodium conductance of the frog node of Ranvier. *J. Gen. Physiol.* 69:915–926.

Sheets. M. F., B. E. Scanley, D. A. Hanck, J. C. Makielski, and H. A. Fozzard. 1987. Open sodium channel properties of single canine cardiac purkinje cells. *Biophys. J.* 52:13–22.

Skenkel, S., E. C. Cooper, W. James, W. S. Agnew, and F. J. Sigworth. 1989. Purified, modified eel sodium channels are active in planar bilayers in the absence of activating neurotoxins. *Proc. Natl. Acad. Sci. USA.* 86:9592–9596.

Sigworth, F. J., and B. C. Spalding. 1980. Chemical modification reduces the conductance of sodium channels in nerve. *Nature (Lond.).* 283:293–295

Smith-Maxwell, C., and T. Begenisich. 1987. Guanidinium analogues as probes of the squid axon sodium pore. Evidence for internal surface charges. *J. Gen. Physiol.* 90:361–364.

Tsien, R. W., P. Hess, E. W. McCleskey, and R. L. Rosenberg, 1987. Calcium channels: mechanisms of selectivity, permeation and block. *Annu. Rev. Biophys. Biophys. Chem.* 16:265–290.

Wang. G. K. 1988. Cocaine-induced closures of single batrachotoxin-activated Na^+ channels in planar lipid bilayers. *J. Gen. Physiol.* 92:747–765.

Woodhull, A. M. 1973. Ionic blockage of sodium channels in nerve. *J. Gen. Physiol.* 61:678–708.

Worley, J. F., III, R. J. French, and B. K. Krueger. 1986. Timethyloxonium modification of single batrachotoxin-activated sodium channels in planar bilayers. Changes in unit conductance and in block by saxitoxin and calcium. *J. Gen. Physiol.* 87:327–349.

Yamamoto, D., J. Z. Yeh, and T. Narahashi. 1984. Voltage-dependent calcium block of normal and tetramethrin-modified single sodium channels. *Biophys. J.* 45:337–344.

Yellen, G. 1987. Permeation in potassium channels: implications for channel structure. *Annu. Rev. Biophys. Biophys. Chem.* 16:227–246.

Yue, D. T., and Marban, E. 1990. Permeation in the dihydropyridine-sensitive calcium channel. Multi-ion occupancy but no anomalous mole-fraction effect between Ba^{2+} and Ca^{2+}. *J. Gen. Physiol.* 95:911–939.